Qubit-photon bound states in superconducting metamaterials

M. Pejić [1], Ž. Pržulj,[1] D. Chevizovich [1], N. Lazarides [2], G. P. Tsironis,[2,3] and Z. Ivić [1,2]

[1]*Laboratory for Theoretical and Condensed Matter Physics, Vinča Institute of Nuclear Sciences, National Institute of the Republic of Serbia, University of Belgrade, P.O. Box 522, Belgrade 11001, Serbia*

[2]*Institute of Theoretical and Computational Physics, Department of Physics, University of Crete, P.O. Box 2208, Heraklion 71003, Greece*

[3]*Department of Physics, Harvard University, Cambridge, Massachusetts 02138, USA*

We study quantum features of electromagnetic radiation propagating in a one-dimensional superconducting quantum metamaterial composed of an infinite chain of charge qubits placed within two stripe massive superconducting resonators. The quantum-mechanical model is derived assuming weak fields and that, at low temperatures, each qubit is either unoccupied or occupied by a single Cooper pair. We demonstrate the emergence of two bands of single-photon qubit bound states with the energies lying outside the photon continuum—one is above and the second slightly below the linear photon band. The higher energy band varies slowly with the qubit-photon center of mass quasimomentum. It becomes practically flat provided that the electromagnetic energy is far below the Josephson energy when the latter is small compared to the charging energy. The dispersion of the lower band is practically identical to that of free photons. The emergence of bound states may cause radiation trapping indicating possible applicability for the control of photon transport in superconducting qubit-based artificial media.

I. INTRODUCTION

During the last two decades, there has been considerable progress in the design of quantum devices based on waveguide structures. The latter is composed of quantum emitters with natural or artificial atoms, i.e., qubits, that are coupled with a one-dimensional (1D) optical channel. Numerous applications in quantum simulation, quantum information processing, and communication have already been discussed in the literature [1–10]. Despite all efforts, the level of control and preservation of quantum coherence achieved in these media is still beyond the requirements for a practical realization of operable quantum information devices. This difficulty could be overcome by a better understanding of the nature of the interaction between matter and radiation. Accordingly, intensive studies of light-matter interaction in waveguide structures are necessary.

Superconducting quantum metamaterials (SCQMMs) are man-made material units that are physically interesting while, additionally, quite promising in the fabrication of quantum devices [11–18]. These engineered media are made of periodically arranged artificial atoms that form superconducting quantum (SCQ) bits while interacting with electromagnetic (EM) fields inside one-dimensional transmission lines (TLs). Owing to spatial confinement, tunability of the SCQ parameters, as well as the ability to tailor the photon dispersion relation in specific setups, SCQMMs may be conveniently engineered to provide tunable "atom"-field interaction that can reach regimes ranging from weak to ultrastrong coupling. This is of particular interest in the case of qubit interaction with quantized radiation fields when strong qubit-photon coupling

leads to effective photon-photon and qubit-qubit correlations. The latter allows for the emergence of interference effects with possible practical applications. For example, photons may exhibit a nontrivial dispersion relation such as band edges and band gaps. Thus quantum metamaterials (QMMs) may be viewed as a photonic crystal [19] with strong potential for practical applications. Additionally, they provide a means for devising comprehensive studies of practical and fundamental aspects of the artificial atom-field interaction.

Investigations of the emergence of atom-photon or qubit-photon bound states [20–32] are of particular importance due to their consequences for radiation propagation [28,33–35], preservation of quantum coherence, and entanglement [32,35,36]. For example, the prohibition of the free propagation of radiation could be attributed to the formation of these bound states. Band generation within the continuum can be used potentially for quantum information storage [28,33,34] and construction of photon memory devices [22]. On the other hand, the recent discovery of topological excitations in SCQMMs implies that, by the engineering of topologically nontrivial QMMs, it would be possible to tackle unavoidable structural irregularities in SCQMMs. This is since the creation of photon-bound states provides the preservation of quantum coherence for times large enough to perform quantum information processing [35]. A further important possible application is the exploitation of qubit-photon bound states in what regards entanglement preservation in quantum information processing [32,36].

In the present paper we study qubit-photon bound states that emerge via the interaction of an EM field propagating through SCQMMs; the latter consist of a massive, two

stripe superconducting resonator filled with a large number ($\mathcal{N} \gg 1$) of Cooper pair box (CPB) or charge qubits. Such an essentially three-dimensional structure differs substantially from the most common realization of SCQ-based waveguiding structures [1] and SCQMM setups [12] in which pointlike SCQs are built-in coplanar resonators. In these two-dimensional architectures, the qubit-photon interaction is described within the Jaynes (Tavis)-Cummings [1] and Dicke model Hamiltonians [29,30]. A realistic theoretical model for the proposed setup is derived in the next section in terms of classical variables, while its quantization is performed in the third section.. It differs substantially from those used in other studies of atom-light interaction in the engineered media so far [29,30], i.e., the modified Dicke Hamiltonian. In particular, while the pure photon part is practically identical to those encountered so far, here the qubit-photon interaction comes from the two-photon processes and has been rarely studied within the cavity and circuit QED.

Analogous two-photon interactions were studied within a quite different context by Fistul and Ustinov [37]. It was shown that the excitation of cavity modes in distributed Josephson junctions (JJs) or parallel arrays of junctions may lead to an enhancement or suppression of the escape rate from the superconducting state. Predicted effects are determined through the applied magnetic field and may be experimentally verified. Additionally, we point to the examples in which one encounters formally equivalent *effective* two-photon interactions, appearing in the model Hamiltonian after the application of dispersive, Schriefer-Wolf–type, unitary transformation to the Rabi, Dicke, and Jaynes-Cummings models. Of particular relevance are theoretical studies of cavity QED systems [2] in the ultrastrong dispersive regime. Finally, an additional example in this direction is provided by a scheme for nondestructive detection of microwave photons [38]. A practical realization is a device based on an ensemble of transmon qubits dispersively coupled to a single resonator.

The paper is organized as follows: Descriptions of the model and the classical Hamiltonian are introduced in Sec. II. The quantization procedure is given in Sec. III. The two-particle Schrödinger equation and its solutions are discussed in Sec. IV. Results and conclusions are summarized in Sec. V. Details of the mathematical derivation are given in the Appendices.

II. EXPERIMENTAL SETUP: THE PROPOSAL

We investigate the nonclassical properties of electromagnetic radiation propagating along the SCQMM in a design visualized in Fig. 1. It is made of an infinite ($\mathcal{N} \rightarrow \infty$), 1D periodic SCQ array, with period ℓ, placed in a TL consisting of two infinite bulk superconductors separated by a distance d; we consider d being of the same order of magnitude as ℓ [15–18] [Figs. 1(a) and 1(b)]. The thickness of the superconducting strips is taken for simplicity to be ℓ. Each SCQ is a tiny superconducting island connected to each bank of the TL through a JJ. The control circuitry for each SCQ [Fig. 1(c)] consists of a gate voltage source V_g coupled to it through a gate capacitor C_g and allows for local control of the SCQMM by altering independently the state of each SCQ [11]. The SCQs exploit the nonlinearity of the Josephson effect and the
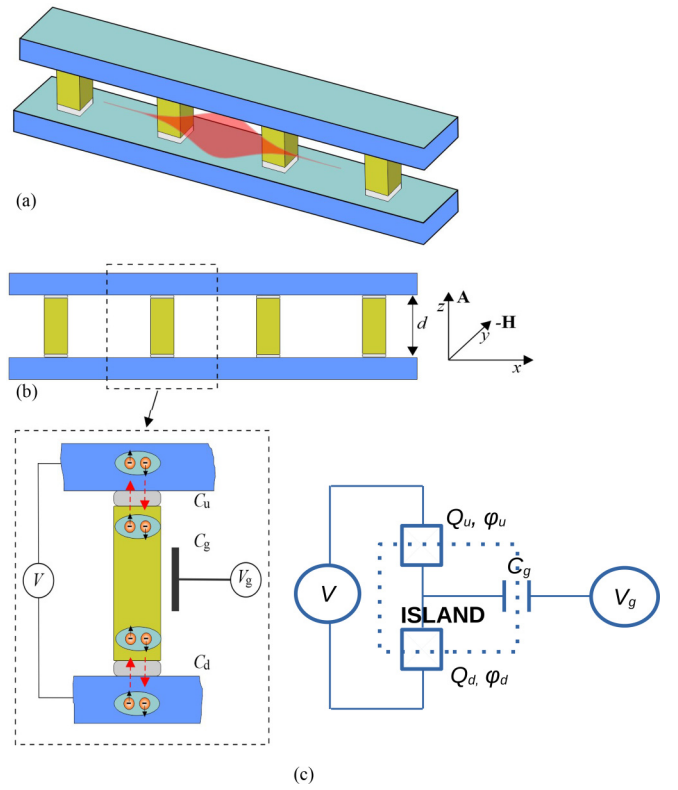

FIG. 1. Illustration of the proposed setup of SCQMM. (a) A chain of Cooper pair box qubits inside the two-stripe transmission line. Each unit cell contains a tiny superconducting island connected with TL banks through two Josephson junctions, for the regions of the dielectric layers (blue). The light-red pulse represents a distribution of the EM field within the device; the vector potential of the propagating EM pulse is shown schematically out of scale. (b) The side view of the SCQMM. The magnetic field penetrates through free space between the islands. (c) Schematic view of the SCQMM unit cell (left pane) and its equivalent scheme (right pane). The tunnel junctions (supposed identical) are connected in series with an isolated island (enclosed in dashes) between them. The control circuitry of the charge qubit consists of a gate potential V_g coupled to a superconducting island through the gate capacitor C_g. V indicates applied voltage on banks. $C_{u,d}$ denotes capacitance of the upper lower JJ, while $Q_{u,d}$ and $\varphi_{u,d}$ denote charges passing through them (u and d) and their conjugated phase differences, respectively. In particular, $\varphi_{u(d)} = \phi_{u(d)} - \phi_m$ stands for the phase difference between the SC order parameters in the upper (lower) bank and SC island.

large charging energy resulting from nanofabrication to create artificial mesoscopic two-level systems.

A. Classical model Hamiltonian

To set up the problem, we first derive the classical model Hamiltonian and subsequently perform its quantization. We assume that an EM wave with vector potential $\vec{A} = A_z(x,t)\hat{z}$ propagates along with the superconducting TL. The direction of propagation is parallel to the superconducting electrodes while $\vec{A}$ is perpendicular to the direction of the EM wave propagation.

The total Hamiltonian is a sum of isolated single unit cell Hamiltonians; the latter is considered to be in the form of

a two junction serially connected JJ segment. In the case when all islands between the neighboring JJs are identical and satisfy the criteria for application of semiclassical approximation, the Hamiltonian of such a multijunction system may be easily deduced employing the straightforward generalization [39] of Feynman's semiclassical treatment of a single JJ [40]. Thus, as sketched in Appendix A4, the two-node truncation of the JJ array Hamiltonian leads to the simple model of two independent JJs [15–18]. In the present case, the semiclassical approximation is not satisfied since the tiny island, the core of the "device," is highly sensitive to charge fluctuations so that even a single Cooper pair (CP) substantially affects the state of the CPB. For that reason, the model Hamiltonian electrostatic energy should be treated appropriately taking into account quantum effects and discreteness of charge in addition to the effects of external voltages and currents. Comprehensive treatment of these effects is far beyond the scope of the present paper. Thus, we shall focus on the main points, discussing, in brief, the impact of applied voltages: the gate (V_g) and bias (V) ones. In the present context, accounting for these effects has no practical importance, since we will restrict ourselves to the unbiased case, also neglecting the gate voltage. In that sense, our treatment here could be understood as an attempt at the consistent foundation of the model and to point out some ways for further work in the framework of more realistic models. In particular, applied voltages and currents may provide the means for external control of the properties of a proposed device. Derivation of the single unit Hamiltonian relies on extensive work on studies of the properties of nanoscale JJs [41–49] used for manipulation of the tunneling of single electrons and Cooper pairs and design of so-called *single electron, Bloch,* and *Cooper pair transistors.*

Single unit Hamiltonian

The equivalent scheme of the single unit cell of our device is represented in Fig. 1(c). The total energy of each of these units consists of the electrostatic and Josephson tunneling energies. The electrostatic energy includes the charging energies of the JJs as well as the energy stemming from the external circuit and gate circuits characterized by the voltages V and V_g, respectively. In Appendix A we give a brief derivation of both energy terms.

The charging energy of the JJ with a certain number of Cooper pairs passing through it is simply that of a charged capacitor. In the absence of external voltages this circuit may be described in terms of charges, Q_u and Q_q on capacitors C_u and C_d, respectively. Alternatively we may use the net charge on the island $q = Q_u - Q_d$ and the total charge Q as *seen from the outside* as defined in Eq. (A2). Both pairs of these variables have their conjugated phases. Thus, one may choose either $\{Q_u, \varphi_u\}$, $\{Q_d, \varphi_d\}$, or $\{Q, \psi\}$ and $\{q, \varphi\}$, where relative phases read $\psi = (\varphi_u + \varphi_d)/2$ and $\varphi = \varphi_u - \varphi_d$. For further convenience, we took the latter possibility and the model Hamiltonian is given by Eq. (A7):

$$H = \frac{Q^2}{4C_\Sigma} + \frac{a^2(n - Q_g/e)^2}{2C_\Sigma} + VQ - 2E_J \cos(\psi/2)\cos\varphi,$$
$$C_\Sigma = C_u + C_d + C_g \equiv 2C_J + C_g. \tag{1}$$

We assume that both junctions are identical, so that $C_u = C_d = C_J$ and $E_J^u = E_J^d$. Introducing the numbers of Cooper pairs (n_u, n_d) passing through the junctions we may express charges (Q and q) as follows: $Q = -e(n_u + n_d)$ and $q = -2e(n_u - n_d) \equiv -2en$. Finally, $Q_g = V_g C_g/2$ stands for the offset charge.

The first term in (1) corresponds to electrostatic energy coming from the total charge across the two JJs connected in series. The second one is the electrostatic energy of the island with the two junctions in parallel, while the third one is the work done by the DC voltage source on the total charge passed through it. The gate charge and corresponding contribution were neglected.

B. Truncated model

In a given moment of time, the system dynamics may be characterized by the number n and its conjugated phase, while Q and ψ represent the external control parameters. Their role will be discussed subsequently. We restrict ourselves to the zero voltage case where the classical system Hamiltonian becomes that of the sum of two noninteracting JJs:

$$H = \sum_{i=l,u} \frac{\hbar^2}{E_c} \dot{\varphi}_i^2 - E_J \sum_{i=l,u} \cos\varphi_i. \tag{2}$$

For convenience, we have reintroduced here the phase differences $\varphi_{u,(d)}$.

In order to express charges with phases we employed the following correspondence: $n_i = -\frac{\hbar C_J}{e^2}\dot{\varphi}_i$. Following [17], we may choose the order parameters of massive superconducting banks as $\phi_d = \phi_u \equiv 0$ so that these phases read $\varphi_u = \phi_u - \phi_m \equiv -\phi_m$ and $\varphi_d = \phi_m - \phi_d \equiv \phi_m$. This choice could be justified in the present special case in the absence of the applied voltages. Otherwise, for example when $V_g \neq 0$, bank phases should be introduced. For example, one may choose $\phi_u = -\phi_d \equiv \phi_0/2$ [41,44], leading to a renormalization of the Josephson energy: $E_J \longrightarrow E_J(\phi_0) = E_J \cos(\phi_0/2)$. Phase ϕ_0 plays the role of control parameter determined by external parameters, V_g in particular.

The energy parameters $E_c = \frac{2e^2}{C_J}$, $E_J = \frac{\Phi_0 I_c}{2\pi c}$, $\Phi_0 = \frac{hc}{2e}$, I_c, C_J, and c are the junction charging energy, so-called Josephson energy, flux quantum, critical current, junction capacity, and speed of light, respectively. In the presence of an EM field Josephson phase difference φ_i acquires the gauge term and reads

$$\varphi_u(t) = -\phi_m - \frac{2\pi}{\Phi_0}\int_1^2 \vec{A}(\vec{r}) \cdot d\vec{l},$$
$$\varphi_d(t) = \phi_m - \frac{2\pi}{\Phi_0}\int_1^2 \vec{A}(\vec{r}) \cdot d\vec{l}. \tag{3}$$

Generalizing (2) to the whole qubit lattice and accounting for the energy of the EM field inside the SCQMM $\{H_{\text{em}} = \frac{1}{8\pi}\int[E_n^2(\vec{r}) + B_n^2(\vec{r})]d^3r\}$ we may derive a total model Hamiltonian.

To facilitate practical calculation we first introduce a dimensionless amplitude of the vector potential $\alpha_n = \frac{2\pi d}{\Phi_0}A_n$. Next we perform an approximate integration in (3): $\int_1^2 \vec{A}(\vec{r}) \cdot d\vec{l} \equiv \frac{2\pi d}{\Phi_0}A_n$. It is justified for the present setup provided that

the separation d between the superconducting stripes and the period ℓ, i.e., the center-to-center distance between qubits, is of the same order of magnitude and much smaller than the wavelength of EM radiation. Under these conditions one may neglect variation of the vector potential within each cell. As a result, the integration in Eq. (3) is trivial (see for example [15–17]). The same approximations were used in evaluating EM energy. Thus, neglecting the spatial variation of an electric and magnetic field within the unit cell, the energy of the EM field, in particular the unit cell, may be approximated as

$$H_{\text{em}} \approx \frac{V}{8\pi}\left(E_n^2 + B_n^2\right),$$
$$V = \ell^2 d, \quad -\text{volume of the unit cell.} \quad (4)$$

Following [15,17] we have neglected the contribution of the electric field, while the fraction that originates from the magnetic field was accounted for through the discretization procedure introduced in [15–17]:

$$B(x,t) = \frac{\partial A(x,t)}{\partial x} \rightarrow \frac{A_{n+1}^z - A_n^z}{\ell}. \quad (5)$$

Here $E_{\text{em}} = \frac{1}{8\pi\ell d}\left(\frac{\Phi_0}{2\pi}\right)^2$ is the so-called electromagnetic energy introduced in [15], determining the speed of "light" in the qubit chain, which, in dimensionless units, reads $\beta = \sqrt{E_{\text{em}}/E_J}$. It, together with the ratio $\gamma = \frac{E_C}{E_J}$, represents the main quantitative characteristic of CPB qubits, their derivatives (transmons for example), and networks made of them. In our analysis the reciprocal value plays the role of qubit-photon coupling constant: $\mu = 1/\gamma \equiv E_J/E_C$.

In accordance with the preceding analysis, the semiclassical Hamiltonian reads

$$H = \sum_n \left[\frac{2\hbar^2}{E_c}\dot{\phi}_n^2 - 2E_J\cos\phi_n\cos\alpha_n \right.$$
$$\left. + \frac{2\hbar^2}{E_c}\dot{\alpha}_n^2 + E_{\text{em}}(\alpha_{n+1} - \alpha_n)^2 \right]. \quad (6)$$

III. QUANTIZATION AND TWO-LEVEL APPROXIMATION

The quantum-mechanical versus (semi)classical description of qubit–EM-field coupled systems still has certain controversies [50]. Nevertheless, at low temperatures, a fully quantum treatment is justified, while the dissipation is negligible. Under these conditions, the quantum state of an island is determined by the number of extra Cooper pairs on them. In addition, EM radiation exhibits quantum features for weak (small amplitude) EM fields when their modes are populated with just a few photons, one or two, per wavelength [51]. At this stage, we must note that the tunneling of the single CP between the banks and island does not affect the state of the former which contains a large number of CPs so the deficiency or the excess of the single CPs has no particular significance. Formally we quantize our model by introducing the photon creation and annihilation operators in real (direct) space and Josephson phase and Cooper pair number operator in a Cooper pair number basis. In such a way, through a few intermediate steps, described in Appendix A, the classical Hamiltonian Eq. (6) can be approximated by the quantum one describing

the interaction of a collection of two-level systems and the quantized multimode electromagnetic field.

A. EM field

In the quantum regime the electromagnetic field is weak, i.e., the dimensionless amplitude of its vector is small and can be treated as quantum fluctuation, i.e., $\alpha_n \rightarrow \hat{\alpha}_n \ll 1$. This enables us to expand $\cos\hat{\alpha}_n \approx 1 - \frac{\hat{\alpha}_n^2}{2}$. Next, we quantize the EM field in two steps: first we define the generalized momentum $P_n = \frac{2\hbar^2}{E_c}\dot{\alpha}_n$ canonically conjugated to α_n. Subsequently we treat photon variables as operators $\alpha_n \rightarrow \hat{\alpha}_n$, $P_n \rightarrow \hat{P}_n$ satisfying the commutation relation $[\hat{\alpha}_n, \hat{P}_m] = i\hbar\delta_{m,n}$. It holds for the transformation Eq. (7) through which we introduce photon creation and annihilation operators in real (direct) space:

$$\hat{\alpha}_n = \frac{1}{2}\sqrt{\frac{E_C}{\hbar\omega}}(a_n + a_n^\dagger), \quad \hat{P}_n = i\hbar\sqrt{\frac{\hbar\omega}{E_c}}(a_n^\dagger - a_n). \quad (7)$$

B. Qubit subsystem

Similarly, in quantization of the CPB qubit subsystem we introduce a pair of canonically conjugated variables (operators): the *phase* $\phi \rightarrow \hat{\phi}$ and Cooper pair number operator $\hat{N} = -i\frac{\partial}{\partial\phi_n}$, $[\phi_n, \hat{N}_n] = i$. Then we rewrite Eq. (6) in the Cooper pair number basis $|N\rangle$, using the correspondence $\hat{N} = -i\frac{\partial}{\partial\phi_n}$ and noticing that $e^{\pm i\hat{\phi}_n}|N\rangle = |N \pm 1\rangle$. Next, in the obtained Hamiltonian we exploit the fact that in *charge and transmon* regimes only the few lowest levels are relevant and we may restrict ourselves to the reduced state space in which the single island can be unoccupied ($N = 0$) or occupied by a single Cooper pair ($N = 1$). The resulting Hamiltonian is nondiagonal in reduced number basis $|0\rangle$, $|1\rangle$, and in the next step we diagonalize the free qubit part by means of transition to the energy eigenbasis ($|e\rangle$, excited state; $|g\rangle$, ground state) performing the norm preserving unitary transformation Eq. (A3). Finally, after neglecting the photon number nonpreserving terms, i.e., those $\sim a_n^2$ and $\sim a_n^{\dagger 2}$, we obtain the quantized model Hamiltonian:

$$H = \Delta\sum_n |e\rangle_n\langle e| + \hbar\omega\sum_n a_n^\dagger a_n - J\sum_n a_n^\dagger(a_{n+1} + a_{n-1})$$
$$+ \sum_n [B(|e\rangle_n\langle g| + |g\rangle_n\langle e|) - A|e\rangle_n\langle e|]a_n^\dagger a_n. \quad (8)$$

Here the first term represents the Hamiltonian of the qubit subsystem with level splitting between the excited- and ground-state $\Delta = 2\epsilon$ ($\epsilon = \sqrt{E_J^2 + E_C^2}$). It is represented here in terms of the operator $|e\rangle\langle e|$ to emphasize that initially the system is prepared so that all qubits are excited. Such atoms are usually called *emitters*. In the pure photon Hamiltonian, the two terms in the second line correspond to the typical boson *tight binding* model describing photon hopping between neighboring qubits. Parameters ω and J stay for the photon frequency and the photon interqubit tunneling amplitude, respectively:

$$\hbar\omega = \sqrt{2E_{\text{em}}E_C + \frac{E_C E_J^2}{\Delta}}, \quad J = \frac{E_{\text{em}}E_C}{2\hbar\omega}. \quad (9)$$

Considering the noninteracting case, pure photon, and qubit system, the present model is analogous to those appearing

frequently in a theoretical description of charge and energy transfer in various contexts. Recent application concerns the photonic band-gap materials where it addresses the photon hopping motion in *coupled resonator (cavities) waveguides* [30,31]. Quantum metamaterials built of such structures with embedded tunable quantum emitters, i.e., qubits, opened a perspective for further development of quantum technological devices, and for studies of nonclassical features of light [51]. Finally, the last term is related to the qubit-photon interaction. It possesses two components: the attractive one, measured by the parameter A, and repulsive $\sim B$:

$$A = \frac{E_J^2 E_c}{4\hbar\omega\epsilon}, \quad B = \frac{E_J E_c^2}{8\hbar\omega\epsilon}. \tag{10}$$

For the convenience we rewrite the interaction Hamiltonian in terms of "atomic" (pseudospin) operators ($\sigma^{\dagger,-,z}$):

$$H_i = \sum_n [B(\sigma_n^\dagger + \sigma_n^-) - A\sigma_n^\dagger \sigma^-] a_n^\dagger a_n. \tag{11}$$

The operators in the attractive interaction term may be rearranged as follows: $\sigma^\dagger \sigma^- a^\dagger a \equiv \sigma^\dagger a \sigma^- a^\dagger - \sigma^\dagger \sigma^-$. Thus, it may be understood to originate on account the simultaneous excitation ($\sigma^\dagger a$) and deexcitation ($\sigma^- a^\dagger$) of the nth qubit by an absorption and emission of the single photon. On the other hand, repulsive interaction comes from the photon scattering by qubits resulting in their excitation ($|e\rangle\langle g|$) and deexcitation ($|g\rangle\langle e|$).

For the comparison, we recall that in coplanar geometry setups [1,2] a qubit-photon interaction may be accounted for within the Dicke and Jaynes-Cummings models in which the coupling term, in rotating wave approximation, reads

$$H_{\mathrm{JC}} = g \sum_n \sigma_n^\dagger a_n + \sigma_n^- a_n^\dagger. \tag{12}$$

Here the qubit-photon interaction is achieved by single-photon processes corresponding to the excitation of a qubit atom in general, by the absorption of the single photon ($|e\rangle\langle g|a$) and vice versa: qubit deexcitation by the emission of a single photon.

Note that here we cannot distinguish whether the interaction is attractive or repulsive. This becomes possible only through deriving the eigenvalue equation, the counterpart of Eq. (21) from the next paragraph, based on the sign of the effective interaction parameter.

So far, the interaction resulting from the setup proposed here was not encountered in the studies of the light-matter interaction either with natural or artificial media. Nevertheless, formally very similar models may appear in solids and magnetic semiconductors [52], when a single electron creates microferromagnetic domains flipping the spins of neighboring ions, while the interaction Hamiltonian is given in terms of the $s - d(f)$ being very similar to (11).

In addition, an effective qubit-photon interaction formally equivalent to the attractive part of (11) appears in a theoretical examination of QED systems [2] by means of the Schriefer-Wolf–type unitary transformation. By analogy with [2] the present setup may be suitable for studies and achievement of qubit readout. We also point out that the studied waveguide is a chain of unit cells [sketched in Fig. 1(b)] each of which contains a single qubit (atom) and may be viewed as an optical

resonator. That is, our waveguide is the set of a large number ($\mathcal{N} \gg 1$) of coupled resonators (unit cells) with one atom per "cavity," which imply translational invariance of the system. Nevertheless, most often, the waveguide is a set of "resonators" designed independently of atoms. In these structures atoms are arranged arbitrarily, depending on the particular application or research subject. Various settings are possible and a particular waveguide may be populated by a few ($\mathcal{N}$) atoms, with one or more atoms per cavity [22–32]. One more distinction must be made in comparison with related systems. In that respect we refer to a quantum metamaterial designed of a coplanar, mostly superconducting, resonator waveguide and several embedded qubits [1–4], where the qubits are linearly[1] coupled to the resonator modes.

IV. QUBIT-PHOTON BOUND STATES

A. Vector of state and the Schrödinger equation

The wave function which diagonalizes Hamiltonian Eq. (8) has the form of a single-photon dressed qubit (atom) state:

$$|\Psi\rangle = \sum_m u_m a_m^\dagger |0\rangle |g\rangle + \sum_{m,n} \Psi_{m,n} \sigma_n^\dagger a_m^\dagger |0\rangle |g\rangle_m,$$

$$\sigma_n^\dagger = |e\rangle_n\langle g|, \quad \Psi_{m,n} = \Psi_{n,m}. \tag{13}$$

Here the probability amplitudes satisfy the normalization condition

$$\sum_m |u_m|^2 + \sum_{m,n} |\Psi_{m,n}|^2 = 1. \tag{14}$$

The first term in state Eq. (8) corresponds to the case when a single photon is excited in site m with probability amplitude u_m, while the qubit remains in its ground state. The second term of a vector of state Eq. (8) corresponds to synchronized excitation of nth qubit and photon at site m. The symmetry property $\Psi_{m,n} = \Psi_{n,m}$ reflects the translational invariance of the chain: solutions must remain invariant when the photon and qubit excitation exchange position in simultaneous excitation of the qubit at site m and the photon at the nth site. Owing to orthogonality of $\langle g|\langle 0|a_m$ and $\langle g|\langle 0|\sigma_m^- a_n$ and $|\Psi\rangle$ we may project Schrödinger equation $H|\Psi\rangle = E|\Psi\rangle$ onto $\sigma_m^\dagger a_n^\dagger |g\rangle |0\rangle$ and $a_m^\dagger |g\rangle |0\rangle$. In this way we obtain a system of coupled equations for the amplitudes $\Psi_{m,n}$ and u_m:

$$(\mathcal{E} - \Delta)\Psi_{m,n} + \frac{J}{2}(\Psi_{m,n+1} + \Psi_{m,n-1} + \{m \rightleftarrows n\})$$

$$= -A\Psi_{m,n}\delta_{m,n} + Bu_m\delta_{m,n},$$

$$\mathcal{E}u_m + J(u_{m+1} + u_{m-1}) = B\Psi_{n,n}. \tag{15}$$

We will solve it by employing Fourier transform. Owing to the translational invariance we pick

$$\Psi_{m,n} = \frac{1}{\sqrt{\mathcal{N}}} e^{i\frac{K(m+n)}{2}\ell} \Phi_{m-n}, \quad u_m = \frac{1}{\sqrt{\mathcal{N}}} \sum_k u_k e^{ikm\ell}. \tag{16}$$

In this way, the second equation in Eq. (15) attains a simple form and may be readily solved for u_m, which then may be

---

[1]The interaction is of the first order in field amplitude and contains only the terms linear in photon operators.

eliminated from the first one. In the resulting equation we employ the translational invariance and take $m - n = l$; next we perform Fourier transform $\Phi_l = \frac{1}{\mathcal{N}^{1/2}} \sum_q \Phi_q e^{iql\ell}$. This finally yields

$$[\mathcal{E} - \Delta + 2J \cos(K\ell/2) \cos \ell q] \Phi_q$$
$$= \left[-A + \frac{B^2}{(\mathcal{E} + 2J \cos K)} \right] \left(\frac{1}{\mathcal{N}} \sum_q \Phi_q \right), \quad (17)$$

where K and q stand for center of mass and relative qubit-photon quasimomenta, while $\mathcal{E} = E - \hbar\omega$. On the basis of this equation it is easy to find the relation for eigenvalues: we first find $\Phi_q = \ldots$, then we multiply both sides of the last equation with $1/\mathcal{N}$ and then sum up both sides over q. This results in

$$1 = \frac{1}{\mathcal{N}} \sum_q \frac{1}{(\varepsilon - \delta + \cos(K\ell/2) \cos q\ell)}$$
$$\times \left[-a + \frac{b^2}{(\varepsilon + \cos K\ell)} \right], \quad (18)$$

where $a = A/2J$, $b = B/2J$, $\delta = \Delta/2J$, and $\varepsilon = \mathcal{E}/2J$ stand for the normalized coefficients. For further convenience we express Eq. (21) in terms of just two parameters, β and γ, which fully characterize the proposed system:

$$a = \frac{1}{4\beta^2} \frac{1}{\sqrt{1 + \gamma^2}}, \quad b = \frac{\gamma a}{2},$$
$$\frac{\hbar\omega}{2J} = 2 + \frac{1}{2\beta^2 \sqrt{1 + \gamma^2}}, \quad (19)$$
$$\delta = 2\sqrt{2 \frac{(1 + \gamma^2)}{\gamma \beta^2} + \frac{\sqrt{1 + \gamma^2}}{2\gamma \beta^4}}.$$

Bound state solutions, if any exist, must lie outside the two-particle continuum (TPC) appearing in the absence of qubit-photon interaction, that is, in accordance with Eqs. (8) and (11) for $(A = B = 0)$. In that case Eq. (17) has solution

$$\varepsilon(q, K) = \delta - \cos q\ell \cos \frac{K\ell}{2}, \quad (20)$$

so that the bound state energy must lie either below the lower energy bound

$$\delta - |\cos(K\ell)/2|$$

or above the higher one:

$$\delta + |\cos(K\ell)/2|.$$

B. Eigenvalue equation

The summation over q may be performed in accordance with the rule $\frac{1}{\mathcal{N}} \sum_q \langle \cdots \rangle = \frac{1}{2\pi\ell} \int_{-\pi/\ell}^{\pi/\ell} dq \langle \cdots \rangle$. This, provided that $|\varepsilon - \delta| > 1$, yields the self-consistent equations for energy eigenvalues:

$$1 = a'(K) \frac{\text{sgn}(\varepsilon - \delta)}{\sqrt{(\varepsilon - \delta)^2 - \cos^2 K\ell/2}},$$
$$a'(K) = -a + b^2 \frac{1}{\varepsilon + \cos K\ell}. \quad (21)$$

Eigenequation (21) is a nonlinear [in $\varepsilon(K)$] transcendental equation and cannot be solved analytically. Nevertheless, its nonlinearity implies that it may have multiple solutions. That is, qubit-photon bound states if any exist should exhibit multi-band structure. To facilitate practical calculations, to examine the possible appearance of multiband structure of the qubit-photon spectra, and finally to compare the present analysis with the related preceding ones [52–54] we rewrite Eq. (21) in the self-consistent form

$$\varepsilon(K) - \delta = \pm \sqrt{a'^2(K) + \cos^2 K/2}, \quad (22)$$

in which, on the right hand side, $\varepsilon(K)$ appears implicitly through $a'(K)$ in accordance with Eq. (21). This "solution" recalls the exact one in the limit $a'(K) \to a$, appearing frequently in different contexts. Examples are numerous, and, despite different physical backgrounds, formally identical solutions may be found in many cases such as *bound states of two photons, phonons, or excitons* [53]. In addition, the problem of the bound state of an impurity atom and its vibrational or magnetic environment [52–54], within the simplest models, also reduces to this elementary solution.

C. Existence of solutions

Solubility of Eq. (21) requires non-negativity of its right hand side; thus, for $\varepsilon - \delta < 0$ ($\varepsilon - \delta > 0$), eigenenergy solutions exist provided that $a'(K) < 0$ [$a'(K) > 0$]. Accordingly, signs ($+$ or $-$) in Eq. (22) stand for $\varepsilon - \delta < 0$ and $\varepsilon - \delta > 0$, respectively. Also, throughout the paper, we may call $a'(K)$ the *effective* qubit-photon interaction strength. The term "effective" is used here to emphasize the self-consistency of (22), and to point to its *formal equivalence* with the exact ones appearing when $a'(K) \to a$. To find $\varepsilon(K)$ we have performed the numerical calculation focusing on the case $\varepsilon - \delta < 0$ when an effective qubit-photon interaction is attractive. An opposite case was not considered since our numerical calculations have shown that the solutions to the eigenvalue problem exist for unrealistic values of system parameters, for example, for $\gamma \approx 100$.

D. Solutions: Analytical considerations

Before presentation of the results of our numerical calculations we perform some auxiliary analytic analysis evaluating explicitly eigenenergies at band edges: $\varepsilon(\pm\pi) \equiv \varepsilon(\pi)$. In that limit (22) becomes

$$\varepsilon(\pi) - \delta = \pm a \left(1 - \frac{a(\frac{\gamma}{2})^2}{\varepsilon(\pi) - 1} \right). \quad (23)$$

The signs ($+$) or ($-$) correspond to $\varepsilon - \delta > 0$ and $\varepsilon - \delta < 0$, respectively. The last equation, in both cases, is the quadratic in $\varepsilon(\pi)$ implying the appearance of two bands, both for attractive and repulsive effective interaction. Solutions of Eq. (23) are

$$\varepsilon_\pm(\pi) = \frac{1 + \delta - a}{2} \pm \frac{1 - \delta + a}{2} \sqrt{1 + \left(\frac{a\gamma}{1 - \delta + a} \right)^2}$$

for the attractive effective interaction,

$$\varepsilon_\pm(\pi) = \frac{1 + \delta + a}{2} \pm \frac{1 - \delta - a}{2} \sqrt{1 - \left(\frac{a\gamma}{1 - \delta - a} \right)^2}$$

for the repulsive one. (24)

For the present setup δ is large as compared with other system parameters. Thus, the ratios in both square roots may be regarded as small quantities. This enables us to expand both square roots in Eq. (24) in terms of "small parameter" $\{a\gamma/[1-(\delta\pm a)]\}^2$ which yields the corresponding asymptotic relations:

$$\varepsilon_- \approx \delta - a - \frac{\left(\frac{a\gamma}{2}\right)^2}{1-\delta+a},$$

$$\varepsilon_+ \approx 1 + \frac{\left(\frac{a\gamma}{2}\right)^2}{1-\delta+a}$$

for the attractive effective interaction, (25)

$$\varepsilon_- \approx \delta + a - \frac{\left(\frac{a\gamma}{2}\right)^2}{\delta+a-1},$$

$$\varepsilon_+ \approx 1 + \frac{\left(\frac{a\gamma}{2}\right)^2}{1-\delta-a}$$

for the "repulsive″ effective interaction.

Based on these equations we may estimate under which conditions particular types of solutions exist. For that purpose, we recall the existence conditions of the solutions (Sec. IV C). We focus on repulsive interaction for which our numerical calculations do not find meaningful solutions for reliable parameter values. According to Eq. (21) its solutions exist provided that $a'(K) > 0$. Substituting the corresponding asymptotic solution from Eq. (24), the third equation in Eq. (25), into $a'(\pi)$ we obtain the following condition:

$$a\left(\frac{\gamma}{2}\right)^2 > \varepsilon(\pi) - 1 \Leftrightarrow \delta + a < 1 + a\left(\frac{\gamma}{2}\right)^2 \text{ for } \varepsilon_+. \quad (26)$$

On the other hand, solution ε_-, after subtracting the δ on both sides, attains the form

$$\varepsilon - \delta = 1 - \delta + \frac{\frac{\gamma^2}{4}}{\delta+a-1}.$$

Note that neither of these conditions can be satisfied in the present case. Namely, the condition for the existence of solutions in the case of repulsive interaction reads $\varepsilon - \delta < 0$, which cannot be satisfied in practice due to large values of δ. In particular, for that purpose $\gamma \gtrsim 100$ is required.

E. Solutions: Numerical results

Numerical calculations were performed for the values of system parameters covering both *charging (large γ)* and *Josephson (small γ)* regimes. In view of coupling strength, i.e., $\mu = 1/\gamma$, charging and Josephson regimes correspond to the weak and strong coupling limit, respectively. Note that, besides $\beta < 1$, there are no particular restrictions on the value of the dimensionless speed of light β in QMM. In particular, in literature [15,16,18,55], β was taken to vary from a few tenths up to 1. Here we restrict ourselves to $\beta \leqslant 0.5$ since the results for its larger values do not exhibit any *substantial qualitative* difference. Thus, we used $\beta = 0.1, 0.2,$ and 0.5, while, for each β, we took four values of coupling constant ranging from weak to strong coupling limit: $\mu = 0.1, 0.2, 1,$ and 5. For the comparison with previous work [53,54] we, in parallel

with current results, present those corresponding to pure attractive interaction, choosing $B = 0$.

Our results are illustrated in Figs. 2–4. The energy spectrum consists of the TPC, green shaded area, and two well-separated bands of qubit-photon bound states (band 1 and band 2). They both appear for each set of system parameters and lie below TPC.

The magnitude of the energies of the band 1 bound states as well as the gap between them and TPC are largest for very small β (Fig. 2). As the coupling constant increases, both the gap and band 1 magnitude increase. At the same time, we observe the band 1 flattening with the rise of the coupling constant, implying the possible slowing down and stopping of qubit-photon bound states. These are general characteristics of energy spectra for all β. To be more specific, qualitatively the same behavior is observed for higher values of β with a somewhat different degree of change.

For example, for $\beta = 0.1$ (Fig. 2) the magnitudes of the band 1 bound state energies and those of the free states, for each K, are almost 20 times higher than for $\beta = 0.5$. In addition, in the strong coupling limit ($\mu = 5$), band 1 is practically indistinguishable from bound states corresponding to pure attractive interaction. As μ decreases band 1 and solutions for the pure attractive interaction separate and both gradually tend towards the TPC.

As presented in the lower part of Figs. 2–4, in parallel with band 1 the second one (band 2) appears. This is the band lying deeply below band 1. It emerges from the competition between the attractive and repulsive interaction and lies below the free photon band. Its dependence on parameters β and μ exhibits similar behavior as for band 1. That is, for large β, irrespective of the values of μ, band 2 and the free photon band are practically identical, due to complete compensation of the effective attractive and repulsive interactions. That is, QMM is fully transparent, and there are no bound states. For smaller values of β attractive interaction dominates over the repulsive and qubit-photon bound states to emerge, provided that γ is high enough. Nevertheless, QMM is still transparent but for qubit-photon bound states.

V. CONCLUDING REMARKS

In this paper, we have studied the energy structure and cooperative qubit-photon excitation of a one-dimensional superconducting quantum metamaterial. The system consists of a large number ($\mathcal{N} \gg 1$) of periodically arranged charge qubits placed inside a massive two-strip superconducting resonator. In such a setup each unit cell of SCQMM [sketched in Fig. 1(b)] can be viewed as an electromagnetic resonator, while the system as a whole represents a coupled-resonator (cavities) waveguide with a single atom per cavity. This setup, upon quantization, exhibits interesting features in comparison to those used so far in the studies of matter-light interaction. In particular, the system is translationally invariant since the number of cavities and atoms match: each cavity contains a single qubit. So far the studies on the subject were carried out under the condition that the individual atoms [22–26,28–32] or their ensembles [27] are placed in different resonators and where translational invariance has been rarely accounted for [32,57]. Furthermore, the qubit-photon interaction is
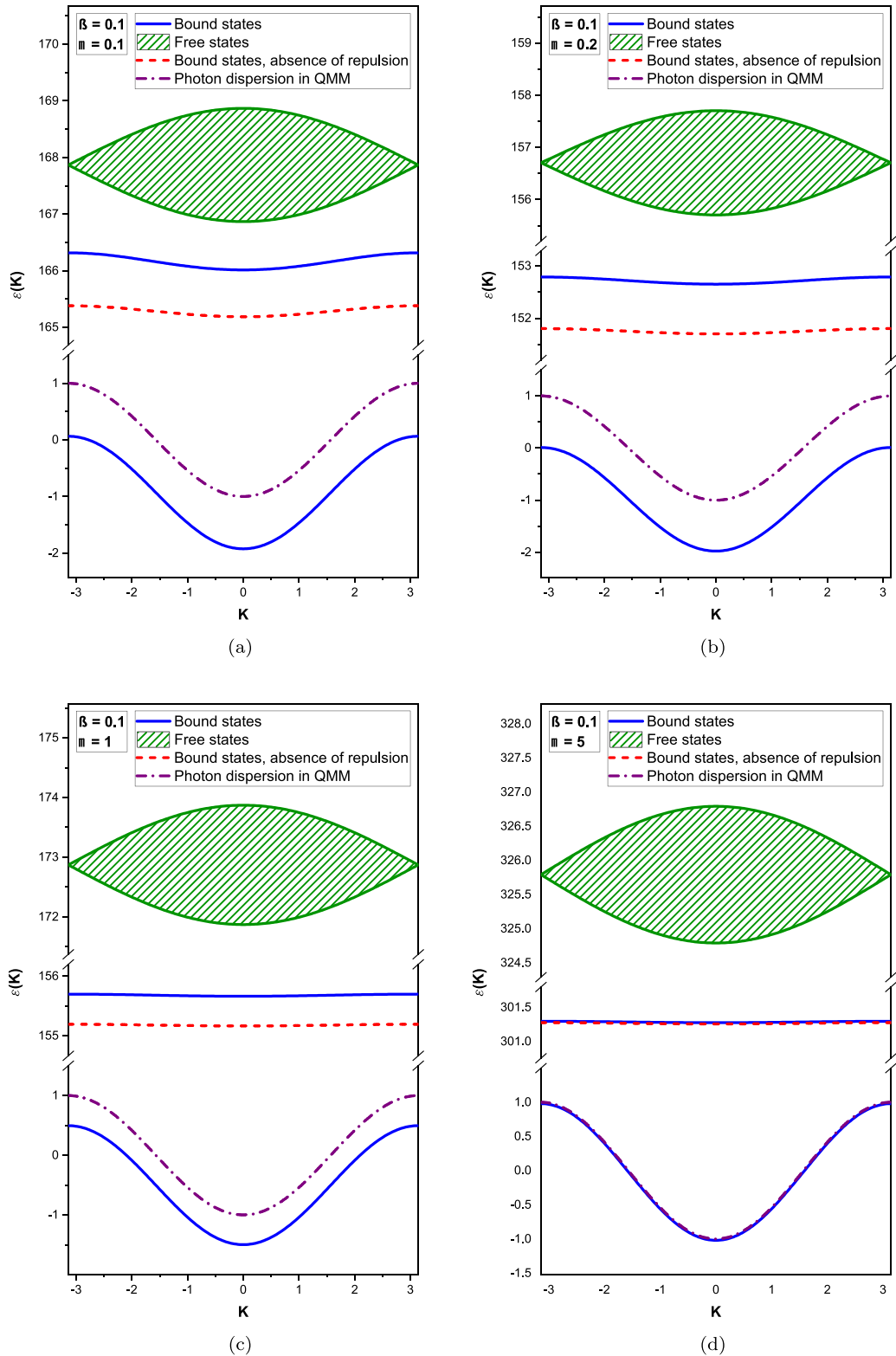
FIG. 2. Graphical illustration of the energy spectrum [$\varepsilon(K)$] of the system for $\beta = 0.1$, and for four different values of μ. The green shaded area corresponds to a two-particle continuum. Blue solid lines correspond to qubit-photon bound states. For comparison we have a band of bound states in the absence of repulsive interaction (red dotted lines) and pure photon dispersion curve $\varepsilon(q)$ (green dotted lines).

substantially different from that utilized in most studies on the subject [22–31] which were carried out within certain modifications of the celebrated Dicke model [56]. The essential difference is that it now has two components, the attractive

and the repulsive one originating on account of different two-photon processes: (i) the attractive one due to simultaneous excitation ($\sigma^\dagger a$) and deexcitation ($\sigma^- a^\dagger$) of the nth qubit by absorption and emission of the single photon and (ii) the
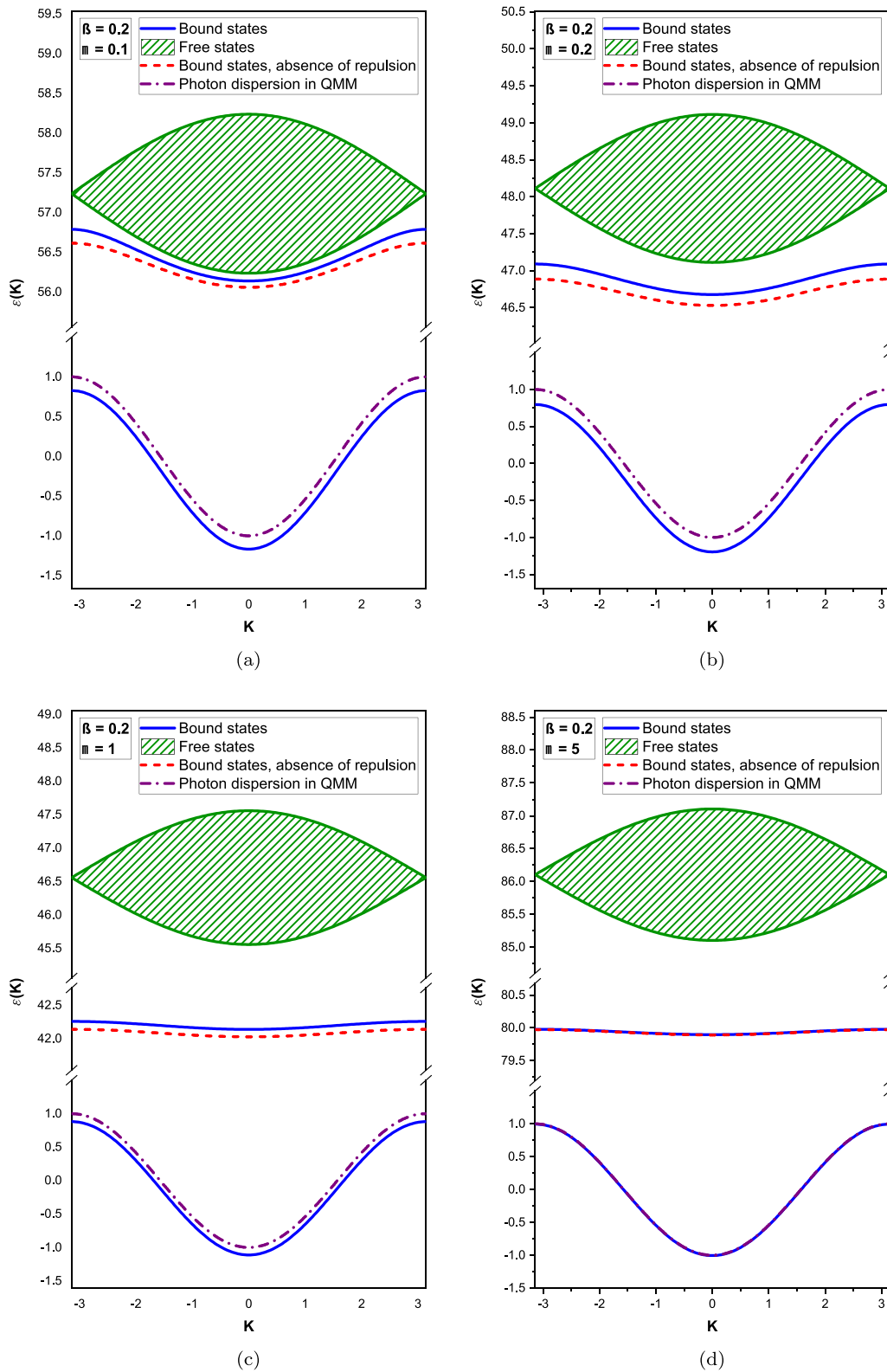
FIG. 3. Energy spectrum $[\varepsilon(K)]$ of the system for $\beta = 0.2$, and for the same values of μ as in the preceding case.

repulsive one from the photon scattering by qubits accompanied by their excitation and deexcitation.

The main consequence of these peculiarities is the emergence of the mixed qubit-photon bound states. In particular, the energy spectrum of the qubit-photon bound states consists of two widely separated bands. The higher energy one lies far over the photon continuum. It is very close to that observed in the simple case of pure attractive interaction and appears for large ε when $a' \rightarrow a$. The results, almost identical to the preceding ones [53,54], were observed. The lower band, near
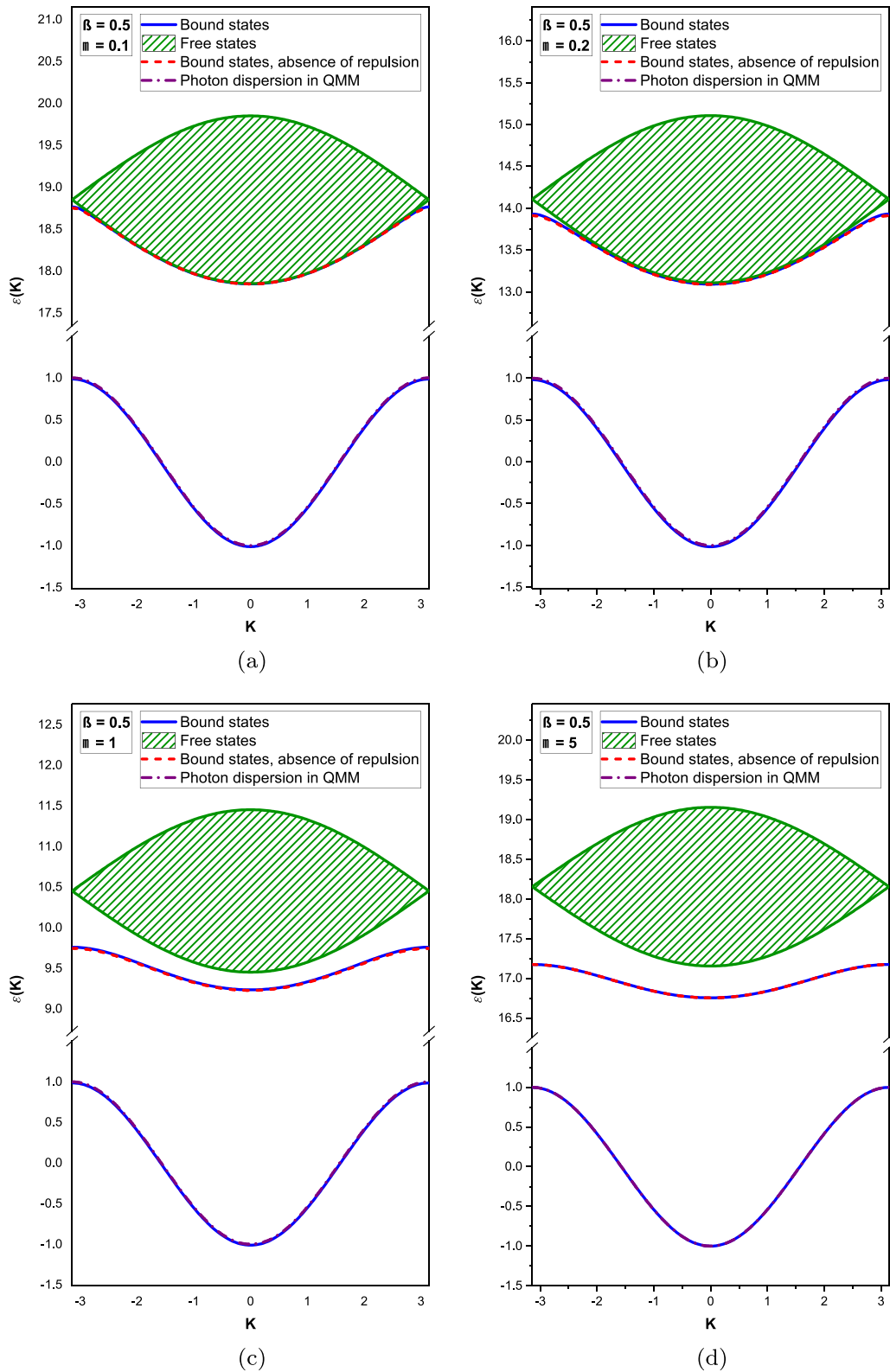
FIG. 4. Same as in previous cases for $\beta = 0.5$.

the band edges, lies within the photon continuum. Based on the recent findings [29,30] we expect that these bound states may exert a considerable influence on the photon transport properties. It relies upon the possibility of radiation trapping due to the creation of these bound states [29,30]. In the present case, due to translational invariance of the system, radiation trapping concerns the qubit dressing by photon cloud. The formation of bands of such complexes implies their free propagation. Band flattening with changes in the values of system parameters points to the slowing down and stopping, in the

final instance, of these mixed states. In such a way, devices based on SCQMM described here could be used for manipulating light propagation and open up a means for realizing operable quantum devices.

The proposed setup is convenient for the practical realization of such devices with controllable parameters which could be achieved by applying external voltages. The simplest way is to attach a gate voltage leading to a renormalization of the Josephson energy: $E_J \longrightarrow E_J \cos \phi_0/2$ with the bank phase playing the role of external control parameter determined by a gate voltage.

Alternatively, one may apply a constant external magnetic field in parallel with a propagating EM field. Thus, both cases may be described by an effective interaction Hamiltonian resulting from (1) after the following redefinition of the dimensionless vector potential $\alpha_n \rightarrow \alpha_n + \alpha_0$. This leads to a modified interaction term in (6):

$$H_i \approx -2E_J \cos \varphi_n \left[\cos \alpha_0 \left(1 - \frac{\alpha_n^2}{2} \right) - \sin \alpha_0 \, \alpha_n \right].$$

Varying external parameters it would be possible to change the tunneling energy and to "flip" between different regimes. A particularly interesting situation arises when $\alpha_0 = \pi/2$ when the interaction term, upon quantization, attains the form identical to that encountered in coplanar arrangements.

Finally, let us comment on the generality of our results. We do not expect that the features of the propagating signal, in the proposed geometrical arrangement, should not qualitatively depend on the particular choice of the type of qubit [11]. Thus, for simplicity and a certain flexibility for the manipulation of the single qubit, we use here charge qubits, while any other type would give analogous results.

APPENDIX A: CLASSICAL MODEL HAMILTONIAN

1. Electrostatic energy

The equivalent scheme of the single unit cell of our device is represented in Fig. 1(c). The Hamiltonian of such a system contains two terms: electrostatic energy and Josephson's coupling term. The electrostatic energy contains the charging energies of the JJs and the ones coming from the

external circuit and gate circuits characterized by the voltages V and V_g, respectively.

The charging energy of the JJ with a certain number of Cooper pairs passing through it is simply that of a charged capacitor. In the absence of external voltages this circuit may be described in terms of charges, Q_u and Q_q on capacitors C_u and C_d. Alternatively, we may use the net charge on the island

$$q = Q_u - Q_d$$

and the total charge Q as seen from the outside. Now we recall [49] that the external circuit sees the two JJs in series as a single capacitor with total capacitance:

$$C = \frac{C_u C_d}{C_u + C_d}. \tag{A1}$$

On the other hand voltage across the junctions is $U = \frac{Q_u}{C_u} + \frac{Q_d}{C_d}$ and may be represented as a ratio of the total charge over the total capacitance $\frac{Q}{C}$. Accordingly, the total charge reads

$$Q = \frac{C_u Q_d + C_d Q_u}{C_u + C_d}. \tag{A2}$$

On the basis of the preceding analysis we obtain a well-known result for electrostatic energy in the absence of applied voltages.

Thus, accounting for both contributions, the electrostatic energy [49] attains a relatively simple form:

$$E_C = \frac{Q_u^2}{2C_u} + \frac{Q_d^2}{2C_d} \equiv \frac{Q^2}{2C} + \frac{q^2}{2(C_d + C_u)}. \tag{A3}$$

The first term here stays for the charging energy of the two seriously connected JJs; the second one corresponds to the electrostatic energy of the island, which sees two JJs in parallel. Accounting for the charge discreteness we may represent charges $Q_{u(d)}$ and q through the corresponding numbers of Cooper pairs $n_{u(d)}$ and elementary unit of charge e: $Q_{u(d)} = -2en_{u(d)}$ and $q = 2e(n_u - n_d)$. External voltages modify the above expressions and give rise to additional electrostatic energy. More precisely, applying gate voltage V_g to the electrode of the gate capacitor attached to the island induces a "gate charge," $Q_g = C_g V_g$. As a result, the net charge on the island is reduced by that amount [7] and now reads

$$q = Q_u - Q_d - Q_g \equiv ne - C_g V_g, \tag{A4}$$

while the island capacitance $C_\Sigma = C_U + C_D + C_G$. Thereby, the gate voltage contribution to electrostatic energy may be accounted by means of (A3) after the substitution $q \rightarrow q - Q_g$ and $C_U + C_D \rightarrow C$.

The external voltage (V) attached to the banks produces another contribution coming from the fact that the whole system behaves like an effective charged particle [total charge Q as given by (6)] in the external voltage so that the electrostatic energy is simply $E_c^{\text{ext}} \sim QV$. As in the case of gate voltage, we have to take $C_U + C_D \rightarrow C_\Sigma$.

2. Josephson tunneling energy

We show that the tunneling part of the Hamiltonian of the double barrier Josephson junction (DBJJ) may be represented simply as a sum of two terms corresponding to
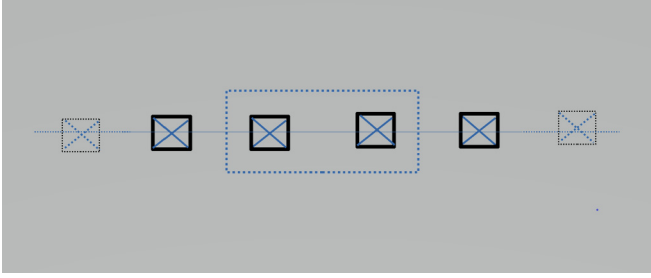
FIG. 5. An array of JJs connected in a series. A two junction segment, corresponding to a single unit cell of SCQMM introduced in Sec. II and represented in Fig. 1, is singled out.

tunneling energy on the particular junction. For that purpose, we employ Feynman's semiclassical theory. We focus on the Josephson part since the electrostatic energy was considered in the preceding subsection. In the case of the DBJJ, three superconducting segments separated by two JJs [Fig. 1(c)]—a wave function in upper, middle, and lower segments—may be written as $\Psi_p(t) = \sqrt{n_p} e^{i\phi_p(t)}$ and $p = u, m, l$, while the tunneling between them now is simply

$$H_t = -K\sqrt{n_u n_u}(\Psi_u^* \Psi_m + \Psi_m^* \Psi_l + \text{c.c.})$$
$$\equiv -K[\cos(\phi_u - \phi_m) + \cos(\phi_m - \phi_d)],$$

where K represents a phenomenological parameter, the so-called Josephson constant [40]. Substituting the CP wave function as given above and, in analogy with [40], assuming that CP numbers in each segment are almost the same and equal to n_0, we found that the interaction (tunneling) Hamiltonian of the double JJ system is the sum of Hamiltonians of two independent JJs:

$$H_t = -K n_0(\cos\varphi_u + \cos\varphi_d) \tag{A5}$$

where parameter $K n_0$ may be identified with Josephson energy.

3. Total classical Hamiltonian

On the basis of the preceding analysis we may write the total model Hamiltonian. Taking that junctions are identical, in terms of pairs $\{Q_u; \varphi_u\}$ it reads

$$H = \frac{Q_u^2 + Q_d^2}{2C_J} + VQ + (Q_u - Q_d)Q_g - E_J(\cos\varphi_u + \cos\varphi_d),$$
$$\tag{A6}$$

while in terms of $\{Q; \psi\}$ and $\{q, \varphi\}$ it is

$$H = \frac{Q^2}{2C_{\text{Tot}}} + \frac{(n - Q_g)^2}{2C_\Sigma} + VQ - 2E_J \cos(\psi/2)\cos\varphi. \tag{A7}$$

4. Classical model Hamiltonian: An alternate derivation

The simplest way to derive the Hamiltonian of a single unit of the qubit chain illustrated in (1) is to view it as an isolated, two junction, segment of a 1D array of a large number of connected JJs [39,46]. Provided that the structure illustrated in Fig. 5 is built of a large number of identical JJs separated

by identical *macroscopic* islands, it may be described by the following Hamiltonian:

$$H = E_c \sum_l \dot{\phi}_l^2 - \sum_{\langle n,m \rangle} E_J \cos(\phi_l - \phi_p), \tag{A8}$$

where $< l, p >$ denotes summation over the nearest neighbors, while E_c and E_J stand for the charging and Josephson energy, respectively. Restricting the whole system to just two JJs (A8) attains the form of two independent JJs.

APPENDIX B: QUANTIZATION OF THE MODEL HAMILTONIAN

1. Quantization of the qubit subsystem

After expansion $\cos\alpha_n \approx 1 - \alpha_n^2/2$, and transition in Cooper pair basis number $|N\rangle$ together with the correspondence $\hat{N} = -i\frac{\partial}{\partial\phi_n}$, and noticing that $e^{\pm i\hat{\varphi}_n}|N\rangle = |N \pm 1\rangle$, we rewrite Hamiltonian Eq. (6) in the charge basis as follows:

$$H = \sum_n 2E_C \hat{N}_n^2 |N\rangle_n\langle N| - E_J \sum_n |N\rangle_n\langle N+1|$$
$$+ |N+1\rangle_n\langle N| + \frac{E_J}{2}\sum_n(|N\rangle_n\langle N+1| + |N+1\rangle_n\langle N|)$$
$$\times \alpha_n^2 + \sum_n\left(\frac{2\hbar^2}{E_c}\dot{\alpha}_n^2 + E_{\text{em}}(\alpha_{n+1} - \alpha_n)^2\right). \tag{B1}$$

In the reduced state space, in which a single island can be unoccupied ($N = 0$) or occupied by a single Cooper pair ($N = 1$), we obtain the reduced Hamiltonian

$$H = -E_c\mathcal{N} + \sum_n\left[E_c\tau_n^z - E_J\tau_n^x\right] + \sum_n$$
$$\times\left(\frac{2\hbar^2}{E_c}\dot{\alpha}_n^2 + E_{\text{em}}(\alpha_{n+1} - \alpha_n)^2 + \frac{E_J}{2}\tau_n^x\alpha_n^2\right) \tag{B2}$$

where $\tau_n^x = |1\rangle_n\langle 0| + |0\rangle_n\langle 1|$ and $\tau_n^z = |1\rangle_n\langle 1| - |0\rangle_n\langle 0|$, while in deriving the above result we have used an apparent relation $\hat{N}_n = |1\rangle_n\langle 1| + |0\rangle_n\langle 0| \equiv 1$. The qubit component of this Hamiltonian may be diagonalized by means of the norm preserving ($1 = |e\rangle_n\langle e| + |g\rangle_n\langle g|$) transformation:

$$\tau_n^x = \cos\eta(|e\rangle_n\langle g| + |g\rangle_n\langle e|) - \sin\eta(|e\rangle_n\langle e| - |g\rangle_n\langle e|),$$
$$\tau_n^z = \cos\eta(|e\rangle_n\langle e| - |g\rangle_n\langle g|) + \sin\eta(|e\rangle_n\langle g| + |g\rangle_n\langle e|),$$
$$\tan\eta = \frac{E_J}{E_C}, \quad \sin\eta = -\frac{E_J}{\sqrt{E_c^2 + E_J^2}}, \quad \cos\eta = \frac{E_C}{\sqrt{E_c^2 + E_J^2}}.$$
$$\tag{B3}$$

In such a way, up to an irrelevant constant, the above Hamiltonian becomes

$$H = \sum_n \left\{ 2\epsilon |e\rangle_n\langle e| + \left[\frac{E_J E_c}{2\epsilon}(|e\rangle_n\langle g| + |g\rangle_n\langle e|) - \frac{E_J^2}{\epsilon}|e\rangle_n\langle e| \right]\alpha_n^2 \right\} + \sum_n \left(\frac{2\hbar^2}{E_c}\dot{\alpha}_n^2 + E_{em}(\alpha_{n+1}-\alpha_n)^2 + \frac{E_J^2}{2\epsilon}\alpha_n^2 \right). \quad \text{(B4)}$$

Here $\epsilon = \sqrt{E_c^2 + E_J^2}$, so that $\pm\epsilon$ denote the ground $(-)$ and excited $(+)$ energy eigenstates.

2. Quantization of the EM field

As usual we consider $\alpha_n \ll 1$ and expand the corresponding "cosine" term in interaction. First we define the generalized momentum $P_n = \frac{2\hbar^2}{E_c}\dot{\alpha}_n$ canonically conjugated to α_n. Now we treat photon variables as operators $\alpha_n \to \hat{\alpha}_n$ and $P_n \to \hat{P}_n$, requiring that they satisfy the commutation relation $[\alpha_n, P_m] = i\hbar\delta_{m,n}$, which holds for the following transformation:

$$\hat{\alpha}_n = \frac{1}{2}\sqrt{\frac{E_C}{\hbar\omega}}(a_n + a_n^\dagger), \quad \hat{P}_n = i\hbar\sqrt{\frac{\hbar\omega}{E_c}}(a_n^\dagger - a_n). \quad \text{(B5)}$$

Substitution of the above expressions in Eq. (A4) yields the following model Hamiltonian:

$$H = \sum_n \left[2\epsilon|e\rangle_n\langle e| + \hbar\omega a_n^\dagger a_n - \frac{E_{em}E_C}{2\hbar\omega}a_n^\dagger(a_{n+1}+a_{n-1}) \right] + \frac{E_J E_C}{8\hbar\omega\epsilon}\sum_n [E_c(|e\rangle_n\langle g| + |g\rangle_n\langle e|) - 2E_J|e\rangle_n\langle e|](a_n^\dagger + a_n)^2,$$

$$H_s = \Delta\sum_n |e\rangle_n\langle e| + \hbar\omega\sum_n a_n^\dagger a_n - J\sum_n a^\dagger(a_{n+1}+a_{n-1}) - \sum_n [A|e\rangle_n\langle e| - B(|e\rangle_n\langle g| + |g\rangle_n\langle e|)a_n^\dagger a_n], \quad \text{(B6)}$$

$$\hbar\omega = \sqrt{2E_{em}E_C + \frac{E_C E_J^2}{\Delta}}, \quad J = \frac{E_{em}E_C}{2\hbar\omega}, \quad A = \frac{E_J^2 E_c}{4\hbar\omega E}, \quad B = \frac{E_J E_c^2}{8\hbar\omega E}. \quad \text{(B7)}$$

[1] Y. Makhlin, G. Schön, and A. Shnirman, Quantum-state engineering with Josephson-junction devices, Rev. Mod. Phys. **73**, 357 (2001).

[2] A. Blais, R. S. Huang, A. Wallraff, S. M. Girvin, and R. J. Schoelkopf, Cavity quantum electrodynamics for superconducting electrical circuits: An architecture for quantum computation, Phys. Rev. A **69**, 062320 (2004).

[3] A. Reiserer and G. Rempe, Cavity-based quantum networks with single atoms and optical photons, Rev. Mod. Phys. **87**, 1379 (2015).

[4] S. Schmidt and J. Koch, Circuit QED lattices: Towards quantum simulation with superconducting circuits, Ann. Phys. (Berlin) **525**, 395 (2013).

[5] S. Ebadi, T. T. Wang, H. Levine, A. Keesling, G. Semeghini, A. Omran, D. Bluvstein, R. Samajdar, H. Pichler, W. W. Ho, S. Choi, S. Sachdev, M. Greiner, V. Vuletić, and M. D. Lukin, Quantum phases of matter on a 256-atom programmable quantum simulator, Nature (London) **595**, 227 (2021).

[6] M. H. Devoret and R. J. Schoelkopf, Superconducting circuits for quantum information: An outlook, Science **339**, 1169 (2013).

[7] N. K. Langford, Circuit QED: Lecture notes, arXiv:1310.1897.

[8] F. Arute, K. Arya, R. Babbush, D. Bacon, J. C. Bardin, R. Barends, R. Biswas, S. Boixo, F. G. S. L. Brandao, D. A. Buell *et al.*, Quantum supremacy using a programmable superconducting processor, Nature (London) **574**, 505 (2019).

[9] I. M. Georgescu, S. Ashhab, and F. Nori, Quantum simulation, Rev. Mod. Phys. **86**, 153 (2014).

[10] H. Bernien, S. Schwartz, A. Keesling, H. Levine, A. Omran, H. Pichler, Soonwon Choi, A. S. Zibrov, M. Endres, M. Greiner, V. Vuletić, and M. D. Lukin, Probing many-body dynamics on a 51-atom quantum simulator, Nature (London) **551**, 579 (2017).

[11] A. M. Zagoskin, in *Quantum Engineering: Theory and Design of Quantum Coherent Structures* (Cambridge University, Cambridge, England, 2011), pp. 1–346.

[12] P. Macha, G. Oelsner, J. M. Reiner, M. Marthaler, S. André, G. Schön, U. Hübner, H. G. Meyer, E. Il'ichev, and A. V. Ustinov, Implementation of a quantum metamaterial using superconducting qubits, Nat. Commun. **5**, 5146 (2014).

[13] P. Jung, A. V. Ustinov, and S. M. Anlage, Progress in superconducting metamaterials, Supercond. Sci. Technol. **27**, 073001 (2014).

[14] N. Lazarides and G. P. Tsironis, Superconducting metamaterials, Phys. Rep. **752**, 1 (2018).

[15] A. L. Rakhmanov, A. M. Zagoskin, S. Savel'ev, and F. Nori, Quantum metamaterials: Electromagnetic waves in a Josephson qubit line, Phys. Rev. B **77**, 144507 (2008).

[16] A. Shvetsov, A. M. Satanin, F. Nori, S. Savel'ev, and A. M. Zagoskin, Quantum metamaterial without local control, Phys. Rev. B **87**, 235410 (2013).

[17] H. Asai, S. Savel'ev, S. Kawabata, and A. M. Zagoskin, Effects of lasing in a one-dimensional quantum metamaterial, Phys. Rev. B **91**, 134513 (2015).

[18] H. Asai, S. Kawabata, S. Savel'ev, and A. M. Zagoskin, Quasi-superradiant soliton state of matter in quantum metamaterials, Eur. Phys. J. B **91**, 30 (2018).

[19] M. Mirhosseini, E. Kim, V. S. Ferreira, M. Kalaee, A. Sipahigil, A. J. Keller, and Oskar Painter, Nat. Commun. **9**, 3706 (2018).

[20] S. John and J. Wang, Quantum optics of localized light in a photonic band gap, Phys. Rev. B **43**, 12772 (1991).

[21] S. John and T. Quang, Photon-hopping conduction and collectively induced transparency in a photonic band gap, Phys. Rev. A **52**, 4083 (1995).

[22] Z. R. Gong, H. Ian, L. Zhou, and C. P. Sun, Controlling quasibound states in a one-dimensional continuum through an electromagnetically-induced-transparency mechanism, Phys. Rev. A **78**, 053806 (2008).

[23] T. Shi and C. P. Sun, Lehmann-Symanzik-Zimmermann reduction approach to multiphoton scattering in coupled-resonator arrays, Phys. Rev. B **79**, 205111 (2009).

[24] Tao Shi, Ying-Hai Wu, A. Gonzalez-Tudela, and J. I. Cirac, Bound states in boson impurity models, Phys. Rev. X **6**, 021027 (2016).

[25] N. M. Sundaresan, R. Lundgren, G. Zhu, A. V. Gorshkov, and A. A. Houck, Interacting Qubit-Photon Bound States with Superconducting Circuits, Phys. Rev. X **9**, 011021 (2019).

[26] G. Calajó, F. Ciccarello, D. Chang, and P. Rabl, Atom-field dressed states in slow-light waveguide QED, Phys. Rev. A **93**, 033833 (2016).

[27] Lei Qiao and Chang-Pu Sun, Atom-photon bound states and non-Markovian cooperative dynamics in coupled-resonator waveguides, Phys. Rev. A **100**, 063806 (2019).

[28] A. Goban, C. L. Hung, S. P. Yu, J. D. Hood, J. A. Muniz, J. H. Lee, M. J. Martin, A. C. McClung, K. S. Choi, D. E. Chang, O. Painter, and H. J. Kimble, Atom-light interactions in photonic crystals, Nat. Commun. **5**, 3808 (2014).

[29] P. Longo, P. Schmitteckert, and K. Busch, Few-Photon Transport in Low-Dimensional Systems: Interaction-Induced Radiation Trapping, Phys. Rev. Lett. **104**, 023602 (2010).

[30] P. Longo, P. Schmitteckert, and K. Busch, Few-photon transport in low-dimensional systems, Phys. Rev. A **83**, 063828 (2011).

[31] C. Vega, M. Bello, D. Porras, and A. González-Tudela, Qubit-photon bound states in topological waveguides with long-range hoppings, Phys. Rev. A **104**, 053522 (2021).

[32] C. Cascio, J. C. Halimeh, I. P. McCulloch, A. Recati, and I. de Vega, Dynamics of multiple atoms in one-dimensional fields, Phys. Rev. A **99**, 013845 (2019).

[33] P. Lodahl, S. Mahmoodian, and S. Stobbe, Interfacing single photons and single quantum dots with photonic nanostructures, Rev. Mod. Phys. **87**, 347 (2015).

[34] P. Lambropoulos, G. M. Nikolopoulos, T. R. Nielsen, and S. Bay, Fundamental quantum optics in structured reservoirs, Rep. Prog. Phys. **63**, 455 (2000).

[35] I. S. Besedin, M. A. Gorlach, N. N. Abramov, I. Tsitsilin, I. N. Moskalenko, A. A. Dobronosova, D. O. Moskalev, A. R. Matanin, N. S. Smirnov, I. A. Rodionov, A. N. Poddubny, and A. V. Ustinov, Topological excitations and bound photon pairs in a superconducting quantum metamaterial, Phys. Rev. B **103**, 224520 (2021).

[36] Q.-J. Tong, J.-H. An, H.-G. Luo, and C. H. Oh, Mechanism of entanglement preservation, Phys. Rev. A **81**, 052330 (2010).

[37] M. V. Fistul and A. V. Ustinov, Quantum cavity modes in spatially extended Josephson systems, Phys. Rev. B **75**, 214506 (2007)

[38] B. Royer, A. L. Grimsmo, A. Choquette-Poitevin, and A. Blais, Itinerant Microwave Photon Detector, Phys. Rev. Lett. **120**, 203602 (2018).

[39] R. P. Douglas, Topics in the theory of Josephson arrays and disordered magnetic systems, Ph.D. dissertation, Ohio State University, 2011.

[40] R. P. Feynman, R. B. Leighton, and M. Sands, *The Feynman Lectures on Physics* (Addison-Wesley, Reading, MA, 1965), Vol. 3, Chap. 21.

[41] K. A. Matveev, L. I. Glazman, and R. I. Shekter, Effects of charge parity in tunneling through the superconducting grain, Mod. Phys. Lett. B **08**, 1007 (1994).

[42] G. Carapella, G. Costabile, R. luca, S. Pace, A. Polcari, and C. Sorino, Josephson equations for the simplest superconducting multilayer system, Physica C **259**, 349 (1996)

[43] M. Tinkham, *Introduction to Superconductivity* (McGraw-Hill, New York, 1996), Chaps. 6 and 7.

[44] A. Zagoskin, *Quantum Theory of Many-Body Systems: Techniques and Applications* (Springer-Verlag, Berlin, 2014), Chap. 4.6.1, pp. 217–223.

[45] D. V. Averin and K. K. Likharev, in *Mesoscopic Phenomena in Solids*, edited by B. Al'tshuler, P. Lee, and R. Webb (Elsevier, Amsterdam, 1991), Chap. 6, Sec. 3.1.

[46] K. K. Likharev, Single-electron devices and their applications, Proc. IEEE **87**, 606 (1999).

[47] G. L. Ingold and Y. V. Nazarov, Charge tunneling rates in ultrasmall junctions, in *Single Charge Tunneling*, edited by H. Grabert and M. H. Devoret (Plenum, New York, 1992), Chap. 2.

[48] A. N. Korotkov, D. V. Averin, K. K. Likharev, and S. A. Vasenko, Single-electron transistors as ultrasensitive electrometers, in *Single Electron Tunneling and Mesoscopic Devices*, edited by H. Koch and H. Lübbig (Springer-Verlag, Berlin, 1992).

[49] H. Grabert, G. L. Ingold, M. H. Devoret *et al.*, Single electron tunneling rates in multijunction circuits, Z. Phys. B **84**, 143 (1991).

[50] J. E. Marchese, M. Cirillo, and N. Grönbech-Jensen, Investigation of resonant and transient phenomena in Josephson junction flux qubits, Phys. Rev. B **79**, 094517 (2009).

[51] S. I. Mukhin and M. V. Fistul, Generation of non-classical photon states in superconducting quantum metamaterials, Supercond. Sci. Technol. **26**, 084003 (2013).

[52] Yu. A. Izyumov, F. A. Kassan-Ogly, and M. V. Medvedev, Magnetic polaron in a ferromagnetic crystal, J. Phys. Colloq. **32**, C1-1076 (1971).

[53] J. C. Kimball, C. Y. Fong, and Y. R. Shen, Anharmonicity, phonon localization, two-phonon bound states, and vibrational spectra, Phys. Rev. B **23**, 4946 (1981).

[54] V. M. Agranovich and O. A. Dubovsky, in *Phonon Multimode Spectra: Biphonons and Triphonons in Crystals with Defects*, edited by R. J. Elliott and I. P. Ipatova, Modern Problems in Condensed Matter Sciences Vol. 23 (Elsevier, Amsterdam, 1988), Chap. 6, p. 297.

[55] Z. Ivić, N. Lazarides, and G. Tsironis, Qubit lattice coherence induced by electromagnetic pulses in superconducting metamaterials, Sci. Rep. **6**, 29374 (2016).

[56] R. Dicke, Coherence in spontaneous radiation processes, Phys. Rev. **93**, 99 (1954).

[57] Lan Zhou, Y. B. Gao, Z. Song, and C. P. Sun, Coherent output of photons from coupled superconducting transmission line resonators controlled by charge qubits, Phys. Rev. A **77**, 013831 (2008).